Developmental Cell
Article

β-catenin Activity in the Dermal Papilla Regulates Morphogenesis and Regeneration of Hair

David Enshell-Seijffers,[1] Catherine Lindon,[1] Mariko Kashiwagi,[1] and Bruce A. Morgan[1,*]
[1]Cutaneous Biology Research Center, Harvard Medical School and Massachusetts General Hospital, Charlestown, MA 02129, USA
*Correspondence: bruce.morgan@cbrc2.mgh.harvard.edu
DOI 10.1016/j.devcel.2010.01.016

SUMMARY

The activity of keratinocytes in the hair follicle is regulated by signals from a specialized mesenchymal niche, the dermal papilla (DP). Here, mice expressing cre recombinase in the DP were developed to probe the interaction between follicular keratinocytes and the DP in vivo. Inactivation of the *β-catenin* gene within DP of fully developed hair follicles results in dramatically reduced proliferation of the progenitors and their progeny that generate the hair shaft, and, subsequently, premature induction of the destructive phase of the hair cycle. It also prevents regeneration of the cycling follicle from stem cells. Gene expression analysis reveals that β-catenin activity in the DP regulates signaling pathways, including FGF and IGF, that can mediate the DP's inductive effects. This study reveals a signaling loop that employs Wnt/β-catenin signaling in both epithelial progenitor cells and their mesenchymal niche to govern and coordinate the interactions between these compartments to guide hair morphogenesis.

INTRODUCTION

Hair follicles undergo cycles of growth (anagen), regression (catagen), quiescence (telogen), and regeneration. During the active growth phase (anagen), the mature hair follicle is composed primarily of keratinocytes arranged in concentric layers of differentiated cell types that comprise the hair shaft (HS), inner root sheath (IRS), and outer root sheath (ORS). Keratinocytes in direct contact with the dermal papilla (DP), a specialized mesenchymal component embedded in the hair bulb at the base of the follicle, undergo asymmetric divisions to renew this "matrix stem cell" compartment and to generate progeny that are displaced away from the DP and undergo a few divisions before differentiating to form the constituents of the HS and IRS (Legué and Nicolas, 2005). Growth of the hair occurs as these constituents are added to the base of the inner layers, the IRS and HS, which are extruded through the ORS toward the surface of the skin.

At the end of the anagen phase, proliferation in the hair matrix ceases. Some matrix cells differentiate to form the terminal structure of the hair (club), while the rest apoptose as the catagen phase begins (Ito et al., 2004). Thus while "matrix stem cells" exhibit asymmetric division, self-renewal, and oligopotency, they are a transient population analogous to those more commonly referred to as committed progenitors in other systems. This population will be referred to as Matrix Progenitor cells Abutting the DP (MPADs) to avoid confusion with nominal stem cell populations in the follicle or the suprabasal cells of the matrix sometimes referred to as matrix progenitors. During the catagen phase, the majority of the ORS of the lower follicle undergo apoptosis. The DP is drawn up with the regressing epithelial strand to lie adjacent to the base of the permanent portion of the follicular epithelium, the secondary germ. A quiescent phase of variable length precedes regeneration of the lower follicle. At the onset of a new anagen phase, keratinocytes in the secondary germ adjacent to the DP proliferate and form a new pool of MPADs. The Cd34-positive "follicular bulge stem cells" and possibly other putative stem cell populations repopulate to the secondary germ to sustain follicular regeneration (Ito et al., 2004; Jaks et al., 2008).

DP cells generate signals that regulate the behavior of keratinocytes in the follicle during the hair cycle. Extirpation and grafting studies broadly support a role for reciprocal inductive and instructive signaling between DP and keratinocytes (Ibrahim and Wright, 1977; Jahoda et al., 1984, 1993; McElwee et al., 2003), but the physical disruption of follicles involved in such studies complicates their interpretation. The fact that many of the genetic pathways active in the DP are either required in mesenchymal cells for the formation of the follicle during embryogenesis or are active in keratinocytes of the follicle as well has hampered the analysis of gene function in the DP. In the absence of an experimental approach to manipulate gene activity in the DP of follicles that have already undergone normal development, it has not been possible to distinguish whether the phenotypic consequences of genetic perturbation result from the indirect consequences of earlier abnormalities in hair follicle development or from ongoing roles of the DP in regulating keratinocyte behavior.

Wnt/β-catenin signaling plays important roles in hair follicle morphogenesis and regeneration. Ablation of *β-catenin* in embryonic epidermis prevents hair follicle formation, whereas forced expression of constitutively activated β-catenin in the epidermis results in expansion of hair follicle fate during development (Huelsken et al., 2001; Zhang et al., 2008) and de novo formation of hair follicles in adults (Gat et al., 1998; Lo Celso et al., 2004). Wnt/β-catenin signaling also plays critical roles in the activation of keratinocytes in the permanent follicle to initiate hair follicle regeneration (Lowry et al., 2005; Van Mater et al., 2003). In addition, β-catenin signaling is active in the keratinocytes of the hair bulb and specifies the differentiation of a subset of their descendents into cell types of the HS (Merrill et al., 2001).

Whereas the direct role of β-catenin signaling in the keratinocyte compartment is established, the function of this pathway in the DP is less clear. Activation of β-catenin in the mesenchyme during dermal development is observed before the initiation of follicle formation and precedes the activation of this pathway in the epidermis (Noramly et al., 1999; Zhang et al., 2009). Pathway activity is then detected in the dermal condensate, a transient mesenchymal compartment that differentiates into the DP (DasGupta and Fuchs, 1999; Zhang et al., 2009). The failure to detect activity of the pathway by reporter assays at later stages and tissue recombination studies with Lef-1-deficient mesenchyme have been taken as evidence suggesting the pathway is inactive in mature DP (DasGupta and Fuchs, 1999; Kratochwil et al., 1996). However, the question of whether activation of the pathway in the DP is sustained during the anagen phase has remained controversial (Maretto et al., 2003).

To directly test the function of specific gene pathways in the DP, mouse strains that allow genetic manipulation in these cells within the context of fully-formed hair follicles in vivo were developed. These were used to analyze the role of β-catenin signaling in the DP of the anagen follicle. Here we report that sustained β-catenin function in the DP is required throughout the growth phase to maintain proliferation of adjacent MPADs and their progeny and to direct HS morphogenesis, in part by regulating the expression of secreted growth factors that can influence keratinocyte behavior. While there is no apparent requirement for β-catenin in the DP during the catagen and telogen stages, regeneration of the follicle from stem cells in the permanent portion of the follicle is also defective in these mice.

RESULTS

DP-Specific Expression of Cre Recombinase

Sequences encoding cre recombinase were inserted into the *Corin* gene locus to generate *Cor-cre* mice. Within the skin, *Corin* is specifically expressed in the DP (Enshell-Seijffers et al., 2008). Disruption of the *Corin* gene does not alter hair follicle development or cycling, although mice homozygous for a *Corin* mutation have increased pheomelanin production on an Agouti background (Enshell-Seijffers et al., 2008). Although *Corin* transcripts were detected in the DP of wild-type mice from the earliest stages of hair follicle morphogenesis when the DP first forms from the dermal condensate (Enshell-Seijffers et al., 2008), cre activity is not detected until after birth. Cre-mediated activation of the *ROSA26 YFP* reporter (*r26YFP*) (Srinivas et al., 2001) in *Cor-cre/+; r26YFP/+* mice was first observed at P3 (Figures 1A and 1B). At this stage most hair follicles lack cells expressing YFP (Figure 1A), but the number of YFP-positive cells in the DP increases rapidly (Figures 1C–1F), and by P7 YFP is detected in virtually all DP cells of all hair types as well as some cells in the proximal dermal sheath (DS) (Figure 1G). Within the skin, cre activity is largely restricted to the DP/DS, but some YFP-positive cells are found at low frequency in the dermis. This pattern of DP-specific expression of YFP remains unchanged throughout the hair cycle and persists as the mice age (Figures 1H and 1I). In contrast to the highly efficient targeting of DP cells, the rare labeled cells outside the DP are variable in position and number, represent a negligible fraction of the dermis and are unlikely to impact follicle behavior. The fact that cre activity is first observed postnatally renders this *Cor-cre* line a powerful tool to manipulate gene expression in the DP after the formation of hair follicles.

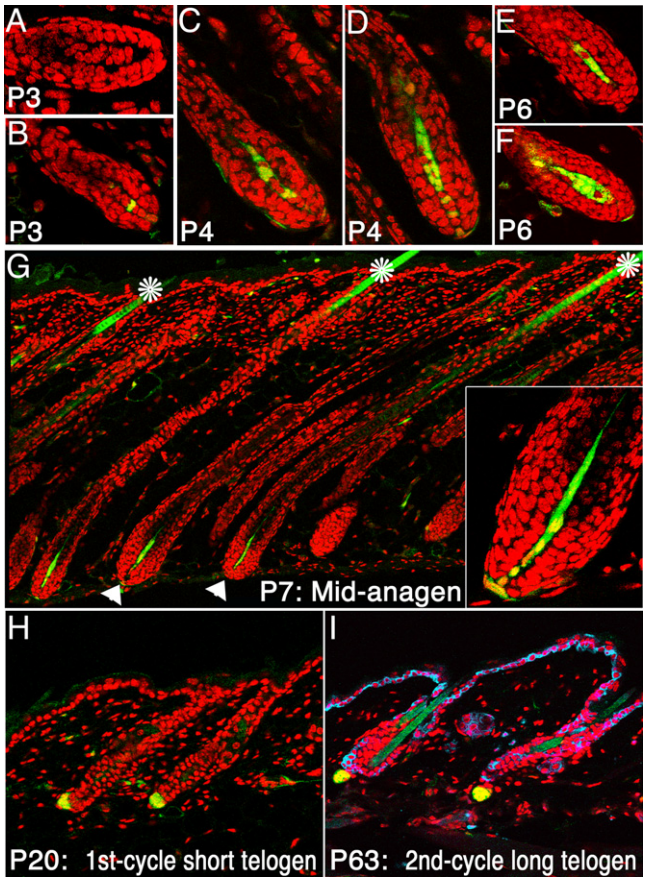

Figure 1. Cre Activity Is Largely Confined to the Dermal Papilla

Cre-mediated activation of the *r26YFP* locus reveals the timing and distribution of cre recombinase activity in *Cor-cre/+; r26YFP/+* mice. YFP (green) was first detected at P3 in some, but not all, follicles (A and B) and increasing numbers of DP cells that express YFP were observed through the midanagen phase (C–F). By P7, virtually all DP cells express YFP (G, arrowheads). Inset in (G) shows higher magnification of a hair bulb. The hair shaft is autofluorescent and its green color is not an indication of cre activity (asterisk). Cre activity remains restricted to the DP as the mice age, as shown during the first (H) and second (I) telogen phases. In (I), K14 staining (blue) labels the basal layer of the interfollicular epidermis and the ORS of the hair follicle. Nuclei are in red.

β-catenin Is Required in the DP for Normal Hair Morphogenesis

The *Cor-cre* line was used to delete a conditional allele of *β-catenin* (Brault et al., 2001) to evaluate the role for β-catenin signaling in regulating follicular keratinocytes indirectly by its action in the DP of the anagen hair follicle. Steps of hair follicle development thought to depend on β-catenin activity, including formation of dense dermis, hair placodes, and DP (Andl et al., 2002), occur in the presence of an intact *β-catenin* gene in mice of the genotype *Cor-cre/+; Ctnnb1*$^{Del/Flox}$*; r26YFP/+*. Deletion of the floxed *β-catenin* allele (*Ctnnb1*^{Flox}) (Brault et al., 2001) to a null allele (*Ctnnb1*^{Del}) occurs in fully functional DP cells during the early to midanagen phase of the hair cycle. Mice

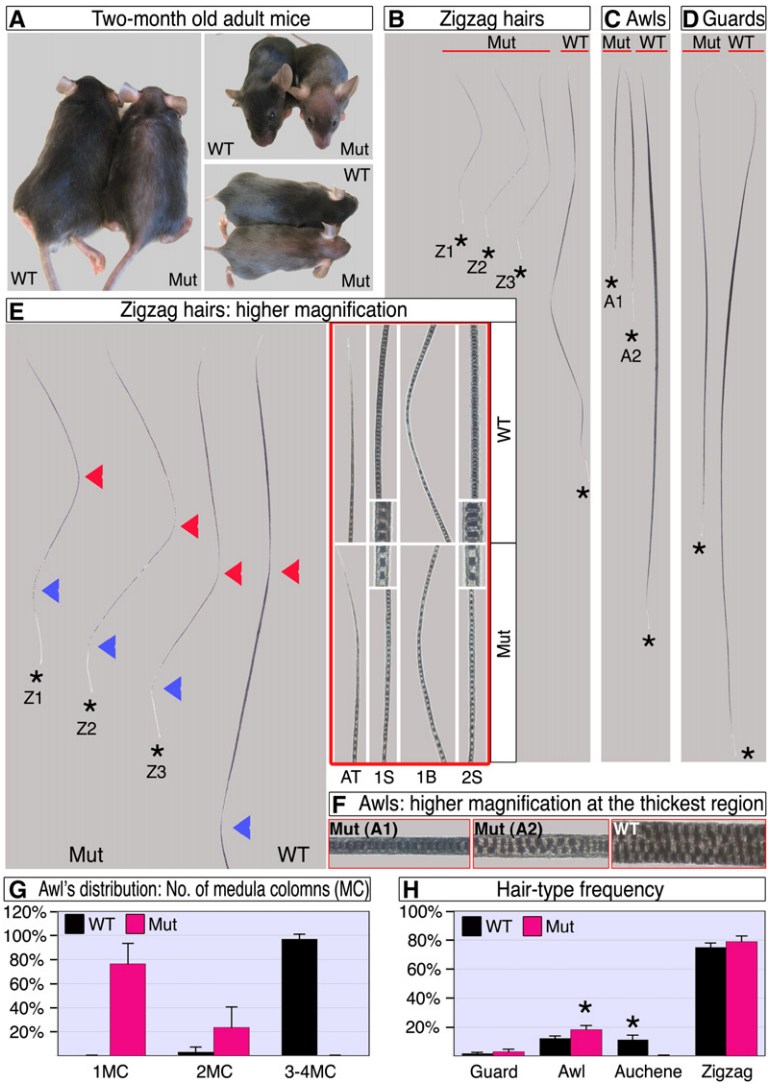

Figure 2. Ablation of *β-catenin* in the DP Results in Dramatic Hair Shortening and Thinning

(A) Adult wild-type and mutant mice. Note that the epidermis is visible through the thin mutant hair coat.

(B–D) Zigzag, awl, and guard hair types after the first hair cycle. The apical tips of all hairs are aligned next to the red line, and hair-clubs are marked by stars. Mutant hairs within a hair type population are classified into subtypes based on their differing lengths and/or thicknesses. Z1–Z3 in (B) represent a first segment that is 50% or less, between 50%–100%, or similar in length to that of wild-type, respectively. A1 and A2 in (C) represent 1 or 2 columns of medulla cells, respectively.

(E) Mutant zigzag hairs and the apical portion of a wild-type zigzag are shown at left. The first and second bends from the apical tip are marked by red and blue arrowheads, respectively. At right, framed with red line, higher magnifications of the apical tip (AT), middomain of the first segment (1S), first bend (1B), and midregion of the second segment (2S) reveal the reduced thickness in mutant hair along the entire hair shaft. Insets show the thickness and organization of the medulla column.

(F) Higher magnifications of the thickest region of awl hairs show the number, structure, and organization of the medulla columns.

(G) Distribution of awl hairs according to the number of medulla columns (MC) at the thickest region (mean ± SD).

(H) Frequency of hair types in wild-type and mutant (mean ± SD). Two-tailed unpaired Student's t test was employed (*$p < 0.0001$).

See also Figure S1.

of the genotype *Cor-cre/+; Ctnnb1*$^{+/Flox}$*; r26YFP/+* or *+/+; Ctnnb1*$^{Del/Flox}$*; r26YFP/+* were phenotypically indistinguishable from wild-type. *Cor-cre/+; Ctnnb1*$^{+/Flox}$*; r26YFP/+* were used as controls throughout this study.

Mouse pelage consists of four hair types with distinctive morphologies. Of the two straight hair types, the long thin guard hairs form first (e14), while the shorter, thicker awl hairs are thought to form in the second wave of folliculogenesis (e16). Auchenes and zigzag hairs are characterized by single and multiple oblique angle bends in the HS, respectively, and are thought to form last (e18). At P5, when YFP expression reveals that cre activity in the DP is becoming prevalent, all follicles are generating HSs, but guard and awl hair follicles have been doing so for longer. When scored at the end of the first hair cycle, all hairs in the mutant pelage are dramatically shorter and thinner than those in wild-type (Figures 2A–2G). Mutant awl hairs are less than half the length of wild-type and are reduced in thickness to a single column of medulla cells from the normal three or four (Figures 2C, 2F, and 2G). Guard hairs are also reduced in length, but less dramatically so, as might be expected from the longer period of growth prior to deletion (Figure 2D).

Zigzag hairs are the most abundant hair type (Figure 2H). In wild-type, these hairs consist of four segments separated by oblique angle bends (Figure 2B). The first segment in mutant hairs varies substantially in length and ranges from 60% to 100% of that observed in wild type, while the second segment is consistently between 50% and 60% of wild-type length (Figures 2B and 2E; Z1–Z3). The third and fourth segments are absent in the mutant. Both remaining segments are thinner than those of the corresponding wild-type.

Auchene hairs, characterized by a single oblique angle bend (see Figure S1 available online), are apparently absent in mutant mice, and the frequency of hairs scored as awls increases (Figure 2H). While this may reflect a role for β-catenin in hair type determination, an alternative and more likely explanation is that changes in the structure of mutant hairs affect the characters used to distinguish these hair types (Figures 2C and 2F; Figure S1). The distal segment of an auchene hair is morphologically indistinguishable from a reduced awl, so premature termination of auchene growth before formation of the single bend would phenocopy awl structure.

Changes in the rate of proliferation in the hair bulb, the duration of the proliferative phase, or both could cause the reduced length of the hair coat. Growth and segmentation of zigzag hairs are not directly coupled, so that the length of individual segments is a good indicator of growth rate, while the number of segments

correlates with the length of the anagen phase of the hair cycle (Hébert et al., 1994; Millar et al., 1999). The structure of the zigzag hairs suggests both proliferation rates and duration of the hair cycle are affected when *β-catenin* is deleted in the DP. The reduced length and thickness of each segment implies proliferation rates are reduced in the mutant, starting shortly after HS formation begins. The variable length of the first segment is consistent with the variable deletion efficiency among follicles predicted by YFP expression at the stage this segment is forming, whereas the more consistent length of the second segment correlates with more uniform deletion predicted by midanagen. The lack of proximal segments suggests that the anagen phase is terminated prematurely.

Compromising *β-catenin* in the DP Reduces Proliferation Rates of MPADs and Their Progeny

At P9, both wild-type and mutant follicles are in the anagen phase and morphologically indistinguishable in skin sections (Figures S2A and S2B). There is no apparent change in DP structure or DP cell numbers, and virtually all DP cells in the mutant express YFP as in littermate controls (Figure S2C). The lack of obvious effect on hair bulb morphology in the mutant may belie underlying molecular alterations that affect hair morphogenesis or simply reflect inefficient deletion of the *β-catenin* gene at this stage. Deletion efficiency was estimated by purifying DP cells from individual mutant and control P9 animals by FACS sorting cells expressing the activated *r26YFP* allele (Figures 3A and 3B). The proportion of YFP-positive cells is similar in wild-type and mutant mice (Figure 3A), confirming the lack of observable alteration in DP cell number or labeling at this stage. Genotyping the sorted YFP-positive cells revealed efficient deletion of the *β-catenin* gene. About 90% of YFP-positive cells lack a functional *β-catenin* gene (Figure 3B and data not shown).

While wild-type and mutant follicles at P10 reveal similar and apparently normal midanagen morphologies (data not shown), analysis of BrdU incorporation in the hair bulb at P10 confirmed that deletion of *β-catenin* in the DP results in decreased proliferation of adjacent MPADs and their immediate progeny (Figures 3C–3F). The number of BrdU-positive cells in the hair bulb is reduced by 67% in mutant follicles.

Alterations of Gene Expression in DP Lacking β-catenin

To identify signals that are regulated by β-catenin activity in the DP compartment, DP cells were purified from mutant and controls at P9 and real-time PCR was employed to evaluate changes in gene expression (Figures 3G–3K). *Axin2* is a direct transcriptional target of the β-catenin pathway and its expression is used as an indicator of pathway activity (Jho et al., 2002). *Axin2* expression in wild-type DP and its 5-fold reduction in mutant DP (Figure 3G) confirm the activity of the β-catenin signaling pathway in wild-type DP cells and its effective reduction in the mutant. β-catenin signaling is often accompanied by the induction of inhibitory factors that negatively modulate the β-catenin pathway. Among these, *Tle1*, *Nkd1*, *Nkd2*, and *Sfrp2* transcripts are also reduced in the mutant DP (Figure 3G), confirming not only that the β-catenin pathway is active in the DP, but that its activity is held in check by negative feedback. Several transcriptional regulators (*Zic1*, *HoxA9*, *Alx3* and *4*, and *Tle1*) also show altered expression in mutant DP (Figure 3I). This raises the possibility that indirect regulation by β-catenin within DP cells may also contribute to cell-autonomous alteration in the expression of signaling genes.

The DP expresses components of several families of intercellular signaling factors known to act on follicular keratinocytes (Rendl et al., 2005). These include BMPs, FGFs, Wnts, and Igfs, as well as secreted proteins that modulate the activities of these signaling molecules. Fgf7, Fgf10, and Igf-1 promote keratinocyte proliferation (Barreca et al., 1992; Greco et al., 2009). Consistent with the observed reduction in matrix cell proliferation, levels of *Fgf7* and *Fgf10* transcripts are dramatically reduced in the mutant DP (Figure 3H), while *Igfbp5* transcripts, which encode a secreted inhibitor of IGF signaling, are increased 4-fold in the absence of β-catenin in DP (Figure 3J).

The BMP and Wnt signaling pathways are also active in matrix keratinocytes. *Wnt5a* is prominently expressed in the DP, but its level is not significantly different when *β−catenin* is deleted in these cells. In DP lacking β-catenin, *Bmp4* expression is unchanged, but the level of *Bmp6* transcripts, which are slightly less abundant than *Bmp4* transcripts in wild-type DP (data not shown), drops 4-fold in the mutant (Figure 3K). Expression of the BMP inhibitor *Gremlin 2* is unchanged, while *Noggin* is reduced 4-fold (Figures 3H and 3K).

Ablation of β-catenin in the DP Results in Premature Induction of Catagen

The length of the anagen phase also contributes to hair length. The duration of anagen was also decreased in the mutant mice (Figure 4). When scored by morphology, catagen onset occurs synchronously in wild-type follicles at P16 (Figure 4C), and follicular regression is largely complete by P19 (data not shown). Catagen onset in the mutant occurs at P12 and is less synchronized. Consequently, a range of follicular morphologies from very early catagen to telogen can be found interspersed in P14 mutant skin, and most follicles are in the telogen phase by P16 (Figures 4B, 4D, and 4E). The number of apoptotic cells in the hair matrix of the follicle is a reliable measure for catagen onset and progression. The distribution of apoptotic cells per hair follicle was analyzed from P10–19 (Figures 4F–4H). This analysis confirms the premature induction of catagen in the mutant.

The appearance of late catagen and telogen follicles by P14 (Figures 4B and 4E) is expected if follicles that entered catagen at P12 progress through this phase at the normal rate. Although the number of apoptotic cells increases more slowly in the mutant when averaged over all follicles (Figure 4H, left), the increase in the number of apoptotic cells during the transition from anagen to mid-catagen is very similar in mutant and wild-type when only those follicles that have entered catagen are scored to eliminate the diluting effects of follicles that remained in anagen (Figure 4H, right). This analysis and the distribution of follicular morphologies observed at successive time points suggest that although the initiation of the regression process is asynchronous and premature, the subsequent progression of individual follicles through the catagen phase to telogen is normal when β-catenin activation is compromised in the DP.

β-catenin Activity in the DP Is Required for Normal Regeneration of the Hair Follicle

Hair follicles in mutant mice assume normal telogen morphology at the end of the premature catagen phase (Figure 4D; Figure S3).

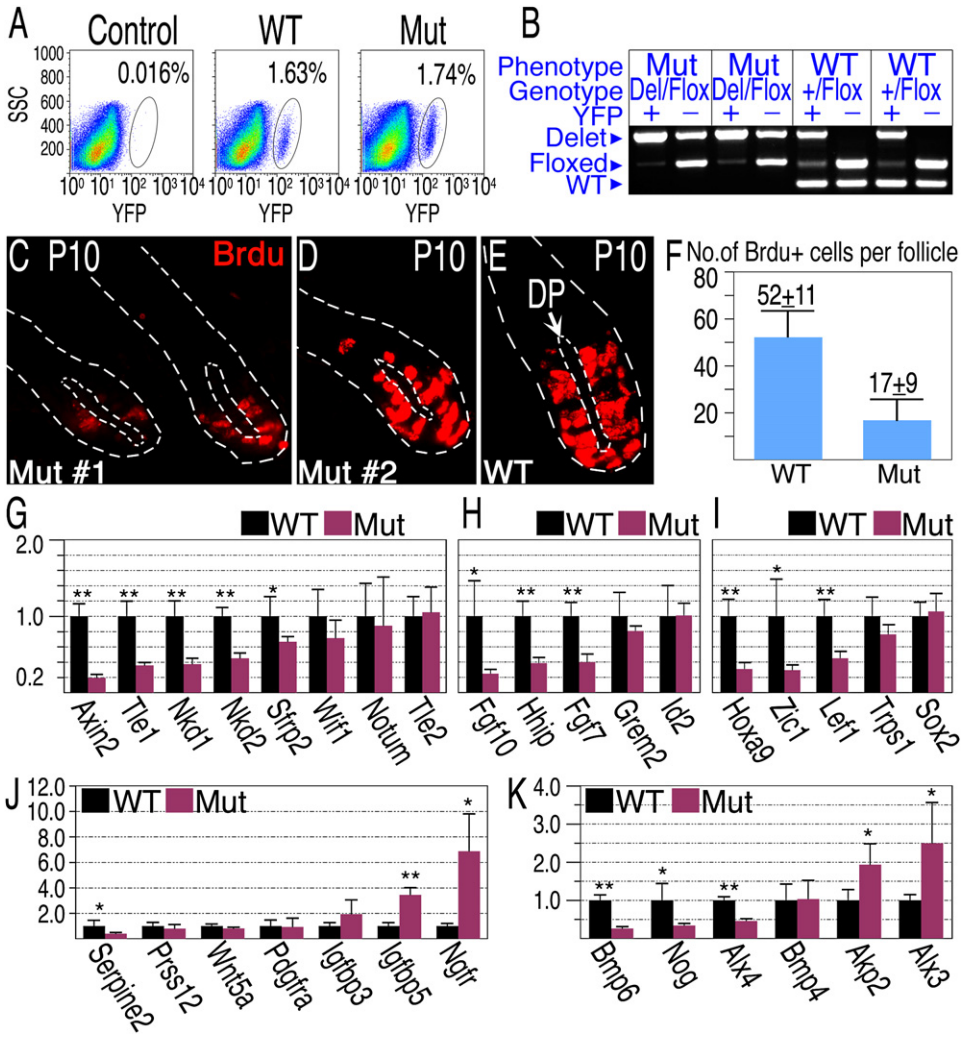

Figure 3. Deletion of *β-catenin* in the DP Results in Reduced Proliferation Rates of Matrix Cells and Alterations of Gene Expression in the DP

(A) FACS analysis of dissociated single cells derived from a back skin of "wild-type" (*Cor-cre/+; Ctnnb1*$^{+/Flox}$ *;r26YFP/+*), mutant (*Cor-cre/+*; *Ctnnb1*$^{Del/Flox}$*; r26YFP/+*), and YFP-negative control (+/+; *Ctnnb1*$^{+/+}$*;r26YFP/+*) P9 mice.

(B) Deletion efficiency of the *β-catenin* gene is 90% at P9. YFP-positive (DP) and YFP-negative (control) cells were FACS sorted from individual mice and used to genotype the *β-catenin* gene. Representative examples at P9 are shown. Note that "wild-type" mice carry one allele of floxed *β-catenin*.

(C–F) BrdU incorporation in P10 mice. Representative examples from two mutants (C and D) and one wild-type (E) are shown to demonstrate BrdU incorporation (red) in the bulb region. The inner and outer dashed lines demarcate the DP and hair follicle, respectively. (F) The average number of BrdU-positive cells in the hair matrix per follicle per section is shown (mean ± SD).

(G–K) Gene expression analysis of Wnt/β-catenin target and DP signature genes. DP cells purified from individual P9 mice were analyzed for gene expression by real-time PCR (mean ± SD; n = 8 for each genotype). The y axis represents fold change in expression with wild-type levels set to 1. Two-tailed unpaired Student's t test was employed (*$p < 0.005$; **$p < 0.0001$). (G) β-catenin target genes known to be involved in a negative feedback loop of the Wnt/β-catenin pathway. (H) Other confirmed and inferred β-catenin target genes. (I and J) Transcriptional regulators (I), secreted factors, and transmembrane receptors (J) known to be expressed in the DP. (K) Components of the Bmp signaling pathway expressed in the DP and Bmp signaling target genes shown to be modulated in the DP in vitro.

See also Figure S2.

Regeneration of the lower follicle is thought to occur in response to an initiating signal from the DP (Sun et al., 1991). Fur was clipped during the first telogen phase to follow the growth of the second hair coat formed by activation of stem cells in the permanent follicle. The clipped region remains largely devoid of hairs in the mutant, with only sparse escaper hairs observed even weeks after the hair coat has completed growth in the controls (data not shown). This defect arises early in the hair cycle. Anagen reentry is normally synchronous in unperturbed mice during the first postnatal hair cycle, and fully regenerated follicles, all at a similar stage of the hair cycle, are observed at P26 in control mice (Figure 5A). Hair follicles in a similar advanced anagen stage are occasionally identified in mutant animals at P26, but these are widely interspersed among follicles exhibiting morphologies characteristic of telogen or an abnormal early anagen phase (Figures 5B–5E).

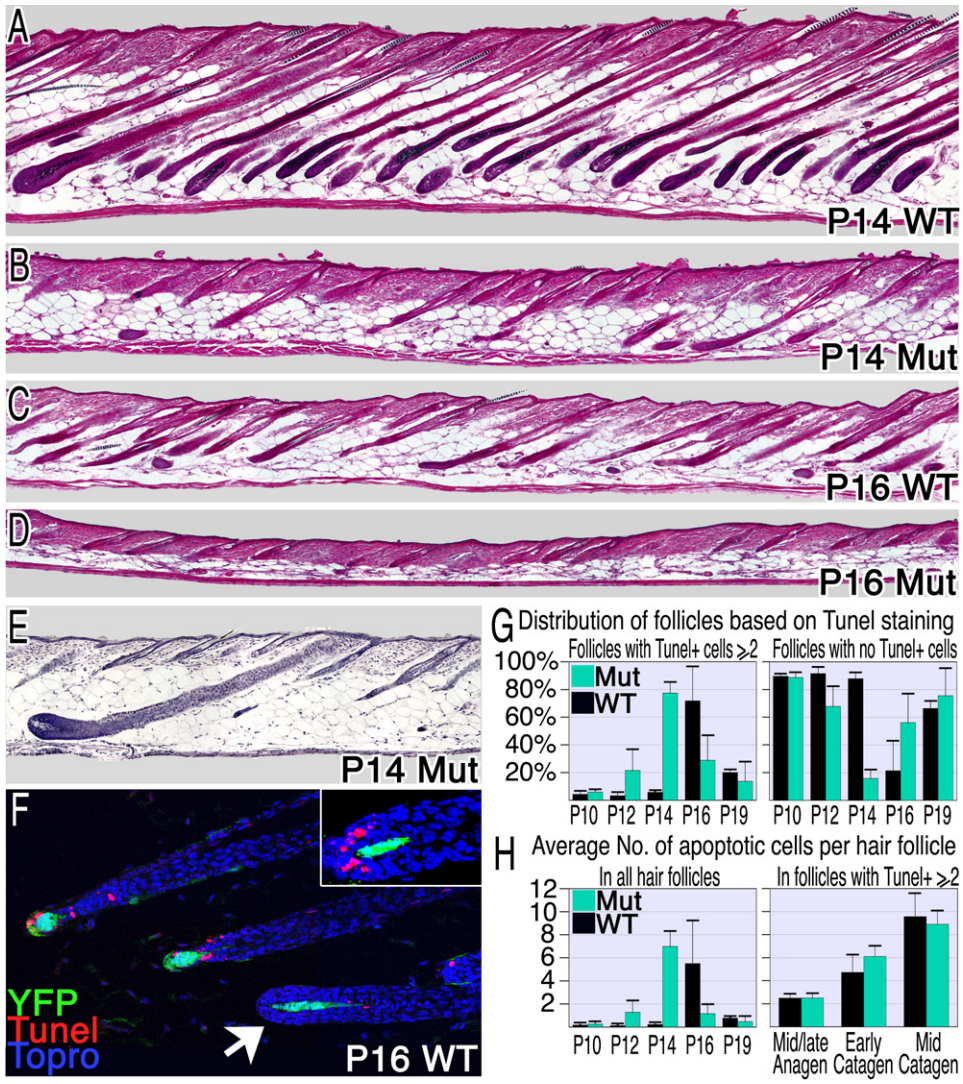

Figure 4. Compromising β-catenin in the DP Induces Premature Catagen

(A–D) Hematoxylin- and eosin-stained sections from wild-type and mutant mice reveal premature and asynchronous induction of the catagen phase in mutant mice.

(E) An anagen follicle surrounded by late catagen and telogen follicles in P14 mutant skin.

(F–H) TUNEL analysis of apoptosis. Follicles in catagen exhibit two or more apoptotic cells, while the absence of apoptotic cells in the hair matrix or bulge was used as a marker for anagen or telogen follicles, respectively (mean ± SD). (F) TUNEL staining (red) of P16 wild-type skin at catagen onset reveals the rapid transition from TUNEL-negative follicles (arrowhead) to those with multiple apoptotic cells/follicle. YFP expression marks the DP (green), and nuclei are blue. Inset shows a follicle morphology typical of the transition from late anagen to early catagen, where abundant TUNEL staining reveals entry to the catagen phase. Many catagen follicles were observed in mutant skin at P12 (G: left), 4 days earlier than wild-type. However, anagen follicles are still predominant at this stage (G: right). (H) The Y axis represents the average number of apoptotic cells per hair follicle per section (mean ± SD). On the left, all follicles were included, and on the right, only those follicles that have entered catagen were scored to eliminate the diluting effects of follicles that remain in anagen.

See also Figure S3.

The failure of regeneration implies either that the signal initiating anagen or the response to it is defective when *β-catenin* is deleted in the DP, or that maturation after anagen onset is blocked. Telogen follicles in the mutant at P50 are morphologically normal, and immunostaining with markers for follicular bulge stem cells (Cd34) and the secondary germ population (P-cadherin) confirms that both populations are present and appear normal (Figure S4). Depilation at P70 can be employed to provide an anagen-inducing signal to the follicles after an extended telogen phase. In wild-type mice, a new hair coat was fully regenerated 20 days after depilation (Figure 5F; Figure S5A). However, when depilation was performed on mutant mice, no hair coat was generated even 40 days after depilation (Figure 5F; Figure S5B). In skin sections from mutant mice 12 days postdepilation, all but a few escaping follicles remained in abnormal early anagen when wild-type follicles had been fully regenerated (Figure S5C). Thus defective progression through the early anagen phase downstream of an anagen-initiating

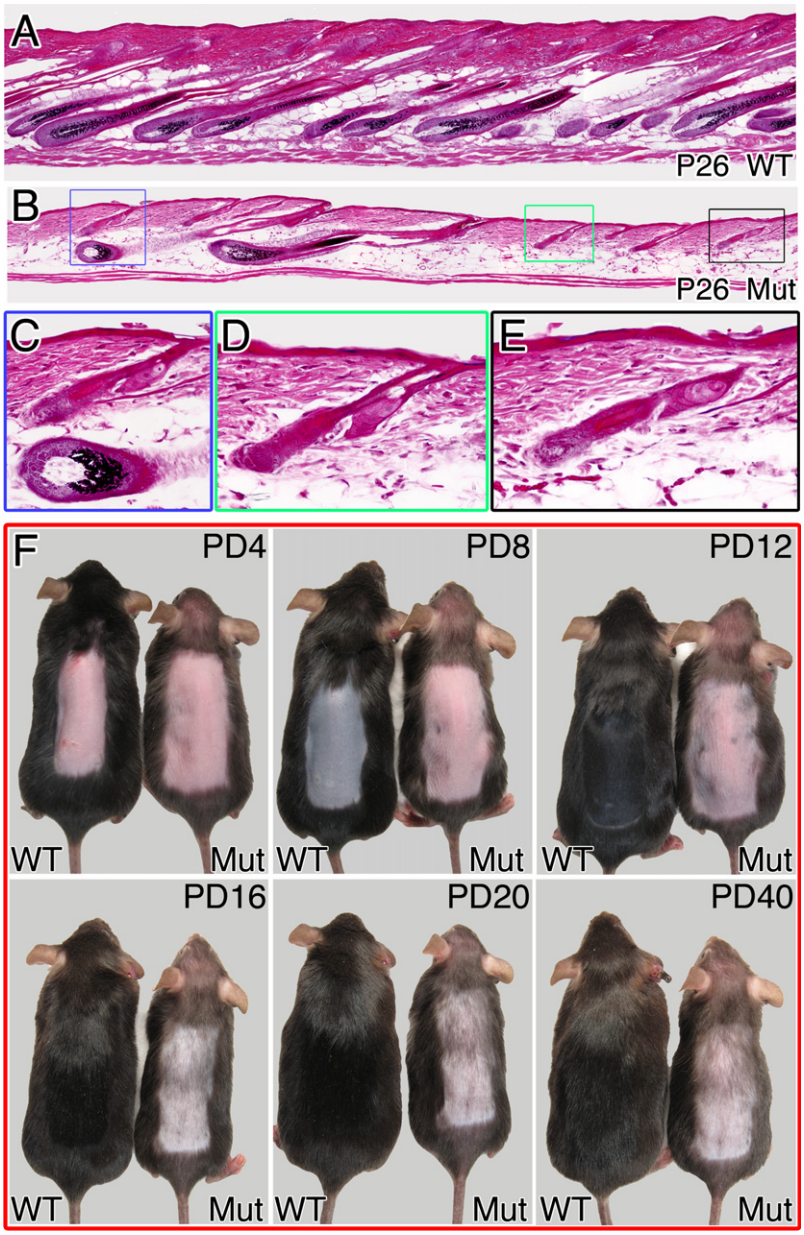

Figure 5. β-catenin Activity in the DP Is Involved in Follicular Regeneration

Hematoxylin and eosin staining of P26 skin sections from wild-type (A) and mutant (B) unperturbed mice. A higher magnification of the colored squares in (B) identifies follicles in advanced anagen (C: lower) and early anagen (C: upper, D, and E) in the same region. (F) Anagen-inducing signal was provided by depilation at P70. Pictures of the same wild-type and mutant mice were taken every 4 days until the hair coat was fully regenerated in the wild-type. Note that in the mutant, the depilated region is largely devoid of hairs with only sparse escapers and this remains unaltered even 40 days postdepilation. PD, postdepilation. See also Figure S5.

signal is largely sufficient to account for the phenotypes observed in the second hair cycle. β-catenin activity in the DP is required for normal regeneration of the hair follicle in both natural and induced hair cycles.

DISCUSSION

While tools to manipulate gene expression in keratinocytes have allowed rapid progress toward characterizing epithelial-mesenchymal interactions at the molecular level from the perspective of the epithelium in this important model system, the lack of tools to alter gene expression specifically in the DP has hampered progress toward defining the role of these cells. The *Cor-cre* line that expresses cre recombinase specifically in the DP after hair follicle formation is an important tool to study the role of the mesenchyme in the hair follicle. By employing this line, we have detected a role for β-catenin in the DP of the hair follicle subsequent to its postulated role in early follicle development. When β-catenin activity is blocked, there is a rapid decrease in the proliferation of adjacent MPADs and their progeny and concomitant reduction in the growth of hair. The maintenance of the transient MPAD pool is also prematurely curtailed. There is no apparent role for β-catenin signaling in the DP during the catagen or telogen phases of the hair cycle. Although the follicular bulge stem cell compartment and secondary germ are apparently unperturbed, the regeneration of the follicle from the stem cell compartment in the permanent follicle is also abnormal in the absence of β-catenin in the DP.

β-catenin Activity and the Hair Cycle

Despite growth effects as early as P5 and efficient deletion of *β-catenin* in the DP by P9, follicles nonetheless remain in anagen until P12. Thus, if β-catenin activity in the DP directly regulates the duration of anagen, either very few DP cells with an intact *β-catenin* gene are sufficient to sustain anagen with reduced proliferation, or there is a significant lag between deletion of the *β-catenin* gene and reduction in the activity of β-catenin-dependent signals required to maintain the anagen phase. Alternatively, the early entry to catagen is a consequence of other alterations in the hair bulb and is not directly regulated by β-catenin activity in the DP. In this context, it is noteworthy that *Nerve growth factor receptor* (*Ngfr*) expression is increased in DP lacking β-catenin (Figure 3J). *Ngfr* mutant mice enter catagen later than wild-type, while overexpression of Ngf in keratinocytes results in premature catagen entry (Botchkarev et al., 2000). Augmented *Ngfr* expression may sensitize mutant DP to a signal promoting catagen.

The synchrony of catagen entry in wild-type skin may be in part due to tissue-wide signals that coordinate activity between follicles. The variable and uncoordinated entry into catagen in the mutant skin suggests that if such signals exist, either the magnitude of their effect is insufficient to overrule follicle-autonomous

influences on the hair cycle, or that the timing of their expression is independent of follicular progression to catagen. In the latter case, they would be expressed too late to influence follicles that had entered catagen autonomously.

Regeneration of the follicle is blocked in mutant mice. The "bulge activation" hypothesis proposes that signals from the DP activate bulge stem cells to initiate anagen (Sun et al., 1991). Depilation either provides or circumvents this initiating signal. Despite this, similarly abnormal regeneration is observed in both depilation and natural hair cycle studies. This confirms a role for β-catenin in the DP very early in the anagen phase, but precludes evaluation of its role, if any, in producing an anagen-inducing signal using the indirect score of hair cycle progression. A molecular definition of anagen initiation will be required for direct evaluation of this question.

β-catenin Regulates Signals from the DP that Orchestrate Keratinocyte Behavior

The data presented here demonstrate that β-catenin is required in the DP of all hair follicle types. Furthermore, all hair types in the mutant are thinner near their distal tips. This suggests that signals from the DP are quantitatively limiting for hair growth, such that blocking production of β-catenin-dependent signals in even a subset of cells within the DP impacts matrix proliferation rates. The variable length of the first segment in mutant zigzag hairs is also consistent with this hypothesis. The first zigzag segment is formed while deletion of *β-catenin* is likely to be variably mosaic in the DPs of different hair follicles.

Among the genes differentially expressed between mutant and wild-type DP, *Fgf7*, *Fgf10*, and *Igfbp5* stand out as likely mediators of the proliferation-promoting activity of the DP during anagen. *Fgf7* expression increases in the DP prior to anagen onset, and exogenous Fgf7 or Fgf10 stimulates proliferation of hair follicle keratinocytes (Greco et al., 2009). Manipulations that impair the function of the Fgf7/10 receptor in keratinocytes result in sparse, thin hair (Grose et al., 2007; Petiot et al., 2003). However, no hair growth phenotype was reported for mice lacking a functional *Fgf7* gene (Guo et al., 1996), and skin grafts from *Fgf10* mutant mice show normal hair growth (Suzuki et al., 2000). This contrasts with the apparent quantitatively limiting nature of signals from the DP and suggests that not only functional redundancy between these Fgfs, but additional feedback mechanisms to regulate growth factor signaling from the DP, would be required to explain these observations. If such feedback exists, disruption of β-catenin in the DP interrupts this regulatory loop.

Igfbp5 was increased in the mutant DP. IGF signaling regulates the size of the HS in vivo and is mitogenic for keratinocytes in vitro. Overexpression of Igf1 in hair follicles increases the size of some HSs and results in a transformation from zigzag to awl-like hairs (Schlake, 2005; Su et al., 1999; Weger and Schlake, 2005). In contrast, forced expression of Igfbp3 or Igfbp5, secreted proteins that decrease Igf1 signaling, results in thinner and slightly shorter hairs (Schlake, 2005; Weger and Schlake, 2005). The increase in *Igfbp5* expression in mutant DP (Figure 3J) may contribute to the reduced hair growth observed in the mutant.

Although the functional importance of Wnt/β-catenin signaling in anagen DP was predicted by our previous in vitro studies, they also suggested the likelihood of context-dependent activity (Kishimoto et al., 2000; Shimizu and Morgan, 2004). In contrast to the result reported here in vivo, in vitro studies using alternative enrichment and culture conditions for DP cells reported decreased expression of *Fgf7* and *Fgf10* when the β-catenin pathway was activated (Rendl et al., 2008). These observations emphasize the importance of performing these studies in the context of an otherwise intact signaling milieu in vivo.

The gene expression analysis presents clear evidence that β-catenin-mediated transcriptional activity plays a critical role in DP cell function. While β-catenin also functions in cell adhesion and adhesion defects could in principle contribute to the phenotype, the morphology of the DP is not discernibly different between wild-type and mutant at any time in the hair cycle, including catagen and telogen when the DP is no longer constrained within the confines of the hair bulb and yet forms a compact ball of cells in intimate contact with the secondary germ (Figure S3). Severe adhesion defects are often accompanied by apoptosis (Frisch and Francis, 1994). However, most follicles in both wild-type and mutant mice are devoid of apoptotic cells in the DP throughout the hair cycle, including the regression phase (Figures S3A and S3B), and the rare apoptotic cells in some DPs during the catagen phase are observed in similar frequency in wild-type and mutant (data not shown).

Signals Acting on the DP

These results suggest that Wnt signaling to the DP regulates its activity. Several Wnts expressed in the hair matrix or differentiating keratinocytes of the proximal follicle have been shown to maintain the inductive properties of enriched DP cell preparations isolated from anagen skin and cultured in vitro. In contrast, the only Wnt known to be expressed in the DP, Wnt5a, was ineffective in this assay (Kishimoto et al., 2000; Shimizu and Morgan, 2004). This suggests that β-catenin activity in the DP is part of a reciprocal signaling loop whereby Wnts expressed in keratinocytes induce activation of β-catenin in the DP to generate the signals that maintain MPAD activity in the anagen phase.

The DP as Niche

The regeneration of the follicle at the end of the telogen phase depends on a stem cell pool in the permanent portion of the follicle. In the prevalent model, signals from the DP activate stem cells resident in the follicular bulge to initiate the production of transient amplifying (TA) cells that then regenerate the follicle (Sun et al., 1991). In this model, the DP may act as a niche for follicular bulge stem cells in the more abstract use of this term by providing a signaling environment conducive to their maintenance and the regulation of their activation, but it is not a physical niche for these cells. Even during the telogen phase, when the DP is closest to the follicular bulge, it remains physically separated from it (Figure S4). In contrast, the DP provides a physical niche for the secondary germ and the MPAD progenitor population that arises from it. At the onset of anagen, a subset of the secondary germ closest to the DP undergoes rapid proliferation and adopts the characteristics of the MPADs that reconstitute the hair bulb. Throughout the anagen phase, physical apposition to DP is one defining character for this

progenitor population that sustains production of the HS and IRS. The work presented here demonstrates that trophic signals regulating MPAD proliferation and maintenance are provided by the DP niche and provides insight into the more general mechanisms that sustain and regulate stem and progenitor cell populations in the adult.

EXPERIMENTAL PROCEDURES

Mice

r26YFP, *β-actin cre*, and conditional knockout allele of *β-catenin* (*Ctnnb1*$^{Flox/Flox}$) strains were obtained from F. Costantini (Columbia), G. Martin (UCSF), and Jackson Labs, respectively. The DP-specific cre (*Cor-cre*) mouse was generated by inserting sequences of cre recombinase into the Corin locus and will be described in detail elsewhere. A knockout allele of *β-catenin* (*Ctnnb1*$^{Del/+}$) was generated by crossing the floxed allele (*Ctnnb1*$^{Flox/Flox}$) to the *β-actin cre* line.

TUNEL and BrdU Analysis

For TUNEL analysis, the In situ cell death detection kit was used (Roche). For BrdU analysis, mice at P10 were injected i.p. with BrdU (100 μg/g body weight) (Molecular Probes). Thirty minutes later, middorsal skins were harvested, fresh-frozen, embedded in OCT, and immunostained with anti-BrdU antibody conjugated with Alexa Fluor 546 (Molecular Probes).

Cell Sorting, Genotyping, and Real-Time PCR

YFP-positive cells were FACS sorted from whole-back skins twice. Purities of about 75% and 95% were obtained after the first and second sort, respectively. To prepare RNA or genomic DNA from sorted cells, the "RNeasy Plus Micro kit" (QIAGEN) and "QAIamp DNA investigator kit" (QIAGEN), respectively, were used. For genotyping, YFP-positive and YFP-negative cells were sorted from the same individual mouse (see Supplemental Information). For gene expression analysis, eight P9 mice per genotype from four different litters were used individually to sort for DP YFP-positive cells. To prepare cDNA, total RNA was reverse transcribed using random hexamer primers and SuperScript III First-Strand synthesis system (Invitrogen). For real-time PCR, primer pairs from SuperArray were employed and differences were quantified based on the ΔΔCt method.

SUPPLEMENTAL INFORMATION

Supplemental Information includes five figures and Supplemental Experimental Procedures and can be found with this article online at doi:10.1016/j.devcel.2010.01.016.

ACKNOWLEDGMENTS

We thank Eleanor Wu and Ying Zheng for technical assistance and F. Costantini and G. Martin for providing mice. This work was supported by grants from the National Institute of Arthritis, Musculoskeletal and Skin Diseases (R01AR055256, B.A.M.), and Shiseido, Ltd. (B.A.M.).

Received: August 24, 2009
Revised: November 24, 2009
Accepted: January 14, 2010
Published: April 19, 2010

REFERENCES

Andl, T., Reddy, S.T., Gaddapara, T., and Millar, S.E. (2002). WNT signals are required for the initiation of hair follicle development. Dev. Cell *2*, 643–653.

Barreca, A., De Luca, M., Del Monte, P., Bondanza, S., Damonte, G., Cariola, G., Di Marco, E., Giordano, G., Cancedda, R., and Minuto, F. (1992). In vitro paracrine regulation of human keratinocyte growth by fibroblast-derived insulin-like growth factors. J. Cell. Physiol. *151*, 262–268.

Botchkarev, V.A., Botchkareva, N.V., Albers, K.M., Chen, L.H., Welker, P., and Paus, R. (2000). A role for p75 neurotrophin receptor in the control of apoptosis-driven hair follicle regression. FASEB J. *14*, 1931–1942.

Brault, V., Moore, R., Kutsch, S., Ishibashi, M., Rowitch, D.H., McMahon, A.P., Sommer, L., Boussadia, O., and Kemler, R. (2001). Inactivation of the beta-catenin gene by Wnt1-Cre-mediated deletion results in dramatic brain malformation and failure of craniofacial development. Development *128*, 1253–1264.

DasGupta, R., and Fuchs, E. (1999). Multiple roles for activated LEF/TCF transcription complexes during hair follicle development and differentiation. Development *126*, 4557–4568.

Enshell-Seijffers, D., Lindon, C., and Morgan, B.A. (2008). The serine protease Corin is a novel modifier of the Agouti pathway. Development *135*, 217–225.

Frisch, S.M., and Francis, H. (1994). Disruption of epithelial cell-matrix interactions induces apoptosis. J. Cell Biol. *124*, 619–626.

Gat, U., DasGupta, R., Degenstein, L., and Fuchs, E. (1998). De Novo hair follicle morphogenesis and hair tumors in mice expressing a truncated beta-catenin in skin. Cell *95*, 605–614.

Greco, V., Chen, T., Rendl, M., Schober, M., Pasolli, H.A., Stokes, N., Dela Cruz-Racelis, J., and Fuchs, E. (2009). A two-step mechanism for stem cell activation during hair regeneration. Cell Stem Cell *4*, 155–169.

Grose, R., Fantl, V., Werner, S., Chioni, A.M., Jarosz, M., Rudling, R., Cross, B., Hart, I.R., and Dickson, C. (2007). The role of fibroblast growth factor receptor 2b in skin homeostasis and cancer development. EMBO J. *26*, 1268–1278.

Guo, L., Degenstein, L., and Fuchs, E. (1996). Keratinocyte growth factor is required for hair development but not for wound healing. Genes Dev. *10*, 165–175.

Hébert, J.M., Rosenquist, T., Götz, J., and Martin, G.R. (1994). FGF5 as a regulator of the hair growth cycle: evidence from targeted and spontaneous mutations. Cell *78*, 1017–1025.

Huelsken, J., Vogel, R., Erdmann, B., Cotsarelis, G., and Birchmeier, W. (2001). beta-Catenin controls hair follicle morphogenesis and stem cell differentiation in the skin. Cell *105*, 533–545.

Ibrahim, L., and Wright, E.A. (1977). Inductive capacity of irradiated dermal papillae. Nature *265*, 733–734.

Ito, M., Kizawa, K., Hamada, K., and Cotsarelis, G. (2004). Hair follicle stem cells in the lower bulge form the secondary germ, a biochemically distinct but functionally equivalent progenitor cell population, at the termination of catagen. Differentiation *72*, 548–557.

Jahoda, C.A., Horne, K.A., and Oliver, R.F. (1984). Induction of hair growth by implantation of cultured dermal papilla cells. Nature *311*, 560–562.

Jahoda, C.A., Reynolds, A.J., and Oliver, R.F. (1993). Induction of hair growth in ear wounds by cultured dermal papilla cells. J. Invest. Dermatol. *101*, 584–590.

Jaks, V., Barker, N., Kasper, M., van Es, J.H., Snippert, H.J., Clevers, H., and Toftgård, R. (2008). Lgr5 marks cycling, yet long-lived, hair follicle stem cells. Nat. Genet. *40*, 1291–1299.

Jho, E.H., Zhang, T., Domon, C., Joo, C.K., Freund, J.N., and Costantini, F. (2002). Wnt/beta-catenin/Tcf signaling induces the transcription of Axin2, a negative regulator of the signaling pathway. Mol. Cell. Biol. *22*, 1172–1183.

Kishimoto, J., Burgeson, R.E., and Morgan, B.A. (2000). Wnt signaling maintains the hair-inducing activity of the dermal papilla. Genes Dev. *14*, 1181–1185.

Kratochwil, K., Dull, M., Farinas, I., Galceran, J., and Grosschedl, R. (1996). Lef1 expression is activated by BMP-4 and regulates inductive tissue interactions in tooth and hair development. Genes Dev. *10*, 1382–1394.

Legué, E., and Nicolas, J.F. (2005). Hair follicle renewal: organization of stem cells in the matrix and the role of stereotyped lineages and behaviors. Development *132*, 4143–4154.

Lo Celso, C., Prowse, D.M., and Watt, F.M. (2004). Transient activation of beta-catenin signalling in adult mouse epidermis is sufficient to induce new hair follicles but continuous activation is required to maintain hair follicle tumours. Development *131*, 1787–1799.

Lowry, W.E., Blanpain, C., Nowak, J.A., Guasch, G., Lewis, L., and Fuchs, E. (2005). Defining the impact of beta-catenin/Tcf transactivation on epithelial stem cells. Genes Dev. *19*, 1596–1611.

Maretto, S., Cordenonsi, M., Dupont, S., Braghetta, P., Broccoli, V., Hassan, A.B., Volpin, D., Bressan, G.M., and Piccolo, S. (2003). Mapping Wnt/beta-catenin signaling during mouse development and in colorectal tumors. Proc. Natl. Acad. Sci. USA *100*, 3299–3304.

McElwee, K.J., Kissling, S., Wenzel, E., Huth, A., and Hoffmann, R. (2003). Cultured peribulbar dermal sheath cells can induce hair follicle development and contribute to the dermal sheath and dermal papilla. J. Invest. Dermatol. *121*, 1267–1275.

Merrill, B.J., Gat, U., DasGupta, R., and Fuchs, E. (2001). Tcf3 and Lef1 regulate lineage differentiation of multipotent stem cells in skin. Genes Dev. *15*, 1688–1705.

Millar, S.E., Willert, K., Salinas, P.C., Roelink, H., Nusse, R., Sussman, D.J., and Barsh, G.S. (1999). WNT signaling in the control of hair growth and structure. Dev. Biol. *207*, 133–149.

Noramly, S., Freeman, A., and Morgan, B.A. (1999). beta-catenin signaling can initiate feather bud development. Development *126*, 3509–3521.

Petiot, A., Conti, F.J., Grose, R., Revest, J.M., Hodivala-Dilke, K.M., and Dickson, C. (2003). A crucial role for Fgfr2-IIIb signalling in epidermal development and hair follicle patterning. Development *130*, 5493–5501.

Rendl, M., Lewis, L., and Fuchs, E. (2005). Molecular dissection of mesenchymal-epithelial interactions in the hair follicle. PLoS Biol. *3*, e331.

Rendl, M., Polak, L., and Fuchs, E. (2008). BMP signaling in dermal papilla cells is required for their hair follicle-inductive properties. Genes Dev. *22*, 543–557.

Schlake, T. (2005). Segmental Igfbp5 expression is specifically associated with the bent structure of zigzag hairs. Mech. Dev. *122*, 988–997.

Shimizu, H., and Morgan, B.A. (2004). Wnt signaling through the beta-catenin pathway is sufficient to maintain, but not restore, anagen-phase characteristics of dermal papilla cells. J. Invest. Dermatol. *122*, 239–245.

Srinivas, S., Watanabe, T., Lin, C.S., William, C.M., Tanabe, Y., Jessell, T.M., and Costantini, F. (2001). Cre reporter strains produced by targeted insertion of EYFP and ECFP into the ROSA26 locus. BMC Dev. Biol. *1*, 4.

Su, H.Y., Hickford, J.G., The, P.H., Hill, A.M., Frampton, C.M., and Bickerstaffe, R. (1999). Increased vibrissa growth in transgenic mice expressing insulin-like growth factor 1. J. Invest. Dermatol. *112*, 245–248.

Sun, T.T., Cotsarelis, G., and Lavker, R.M. (1991). Hair follicular stem cells: the bulge-activation hypothesis. J. Invest. Dermatol. *96*, 77S–78S.

Suzuki, K., Yamanishi, K., Mori, O., Kamikawa, M., Andersen, B., Kato, S., Toyoda, T., and Yamada, G. (2000). Defective terminal differentiation and hypoplasia of the epidermis in mice lacking the Fgf10 gene. FEBS Lett. *481*, 53–56.

Van Mater, D., Kolligs, F.T., Dlugosz, A.A., and Fearon, E.R. (2003). Transient activation of beta -catenin signaling in cutaneous keratinocytes is sufficient to trigger the active growth phase of the hair cycle in mice. Genes Dev. *17*, 1219–1224.

Weger, N., and Schlake, T. (2005). Igf-I signalling controls the hair growth cycle and the differentiation of hair shafts. J. Invest. Dermatol. *125*, 873–882.

Zhang, Y., Andl, T., Yang, S.H., Teta, M., Liu, F., Seykora, J.T., Tobias, J.W., Piccolo, S., Schmidt-Ullrich, R., Nagy, A., et al. (2008). Activation of beta-catenin signaling programs embryonic epidermis to hair follicle fate. Development *135*, 2161–2172.

Zhang, Y., Tomann, P., Andl, T., Gallant, N.M., Huelsken, J., Jerchow, B., Birchmeier, W., Paus, R., Piccolo, S., Mikkola, M.L., et al. (2009). Reciprocal requirements for EDA/EDAR/NF-kappaB and Wnt/beta-catenin signaling pathways in hair follicle induction. Dev. Cell *17*, 49–61.

Developmental Cell 18

Supplemental Information

β-catenin Activity in the Dermal Papilla Regulates Morphogenesis and Regeneration of Hair

David Enshell-Seijffers, Catherine Lindon, Mariko Kashiwagi, and Bruce A. Morgan1

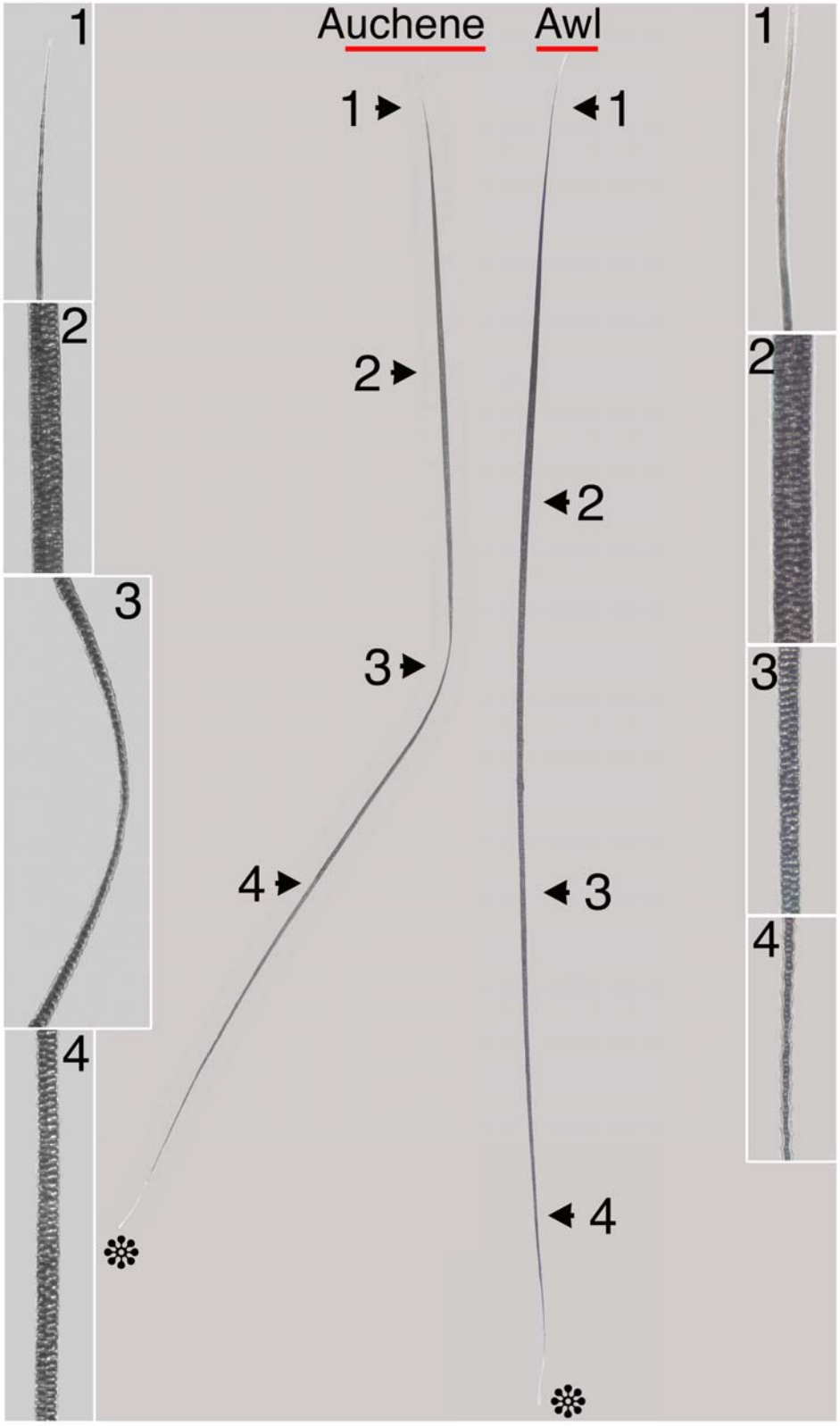

Figure S1. Structural similarity of distal auchene and awl hairs in wild type mice (related to Figure 2)

Awl and auchene wild type hairs are shown with the apical tip aligned next to the red line and the hair club marked by a star. Arrowheads demarcate hair domains shown in higher

magnification in the insets to the right or left of the awl or auchene respectively. An auchene hair is composed of two segments, apical and proximal, that are connected by a single constriction/bend. In contrast, an awl hair is straight with no constrictions or segments. Note the structural resemblance of awl hair to that of the apical segment of auchene hair. In both auchene and awl, the medulla starts with one thin column near the tapered apical tip, increases rapidly to multiple columns and then tapers to single thin column at the constriction or proximal end, respectively. The apparent hair-type transformation from auchene to awl observed in the absence of β-catenin in the DP may be attributed to the structural similarity of these two hair-types in the apical segment and premature termination of hair shaft formation before the generation of the single constriction in auchenes. While thinning of the medulla occurs more abruptly in the apical segment of an auchene than in an awl, the general reduction in medulla thickness would tend to obscure this criterion as well.

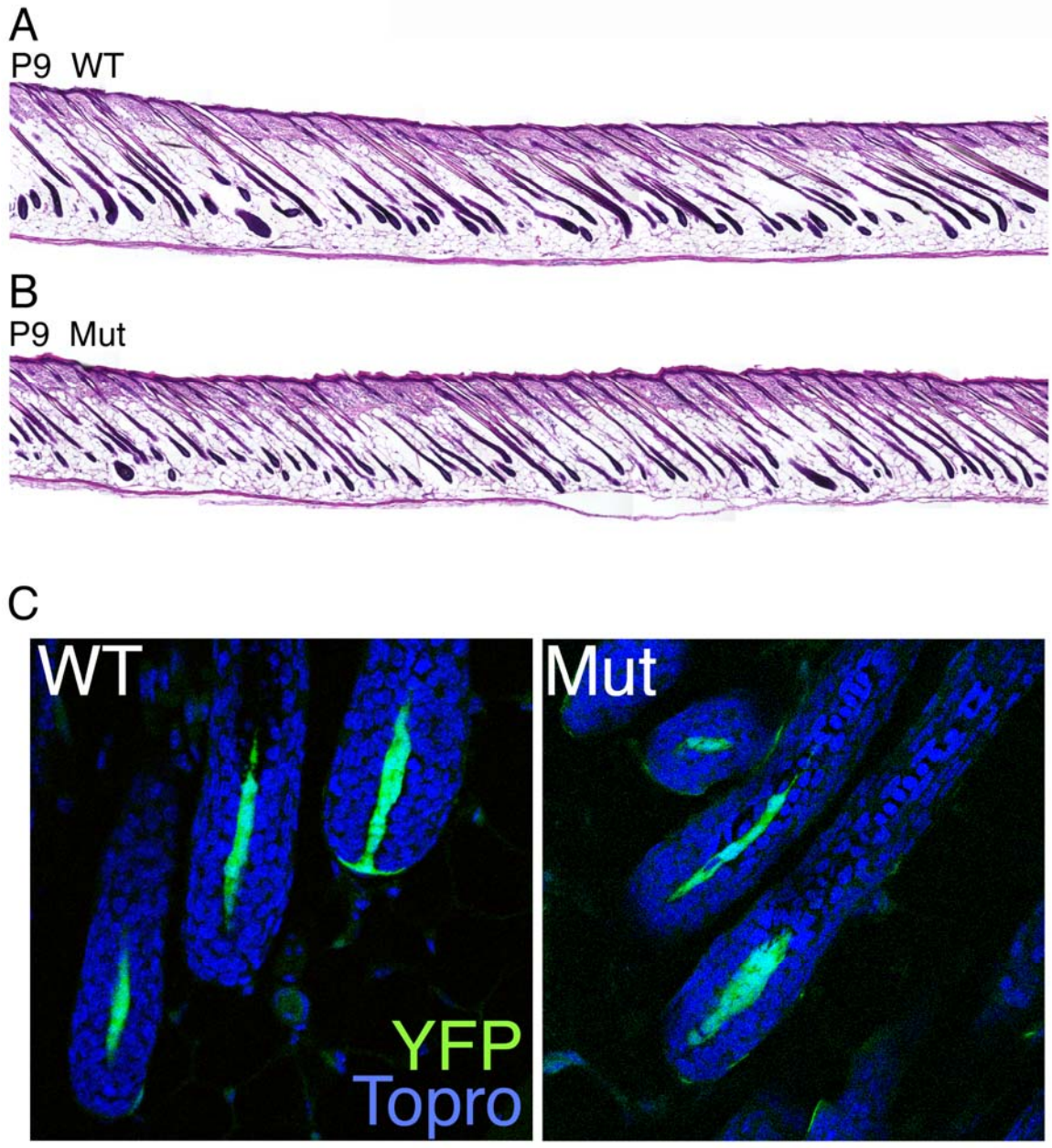

Figure S2. Skin morphology and YFP expression in P9 wild type and mutant littermates (related to Figure 3)

(A,B) Hematoxylin and eosin staining of P9 skin sections from wild type and mutant mice. Note all follicles in the wild type and mutant are in mid-anagen and morphologically similar. (C) Confocal microscopy of YFP expression. Virtually all DP cells express YFP in both the wild type and mutant, indicating that activation of the YFP reporter allele remains highly efficient even when the number of floxed alleles within the same cell increases. Nuclei-blue, YFP-green.

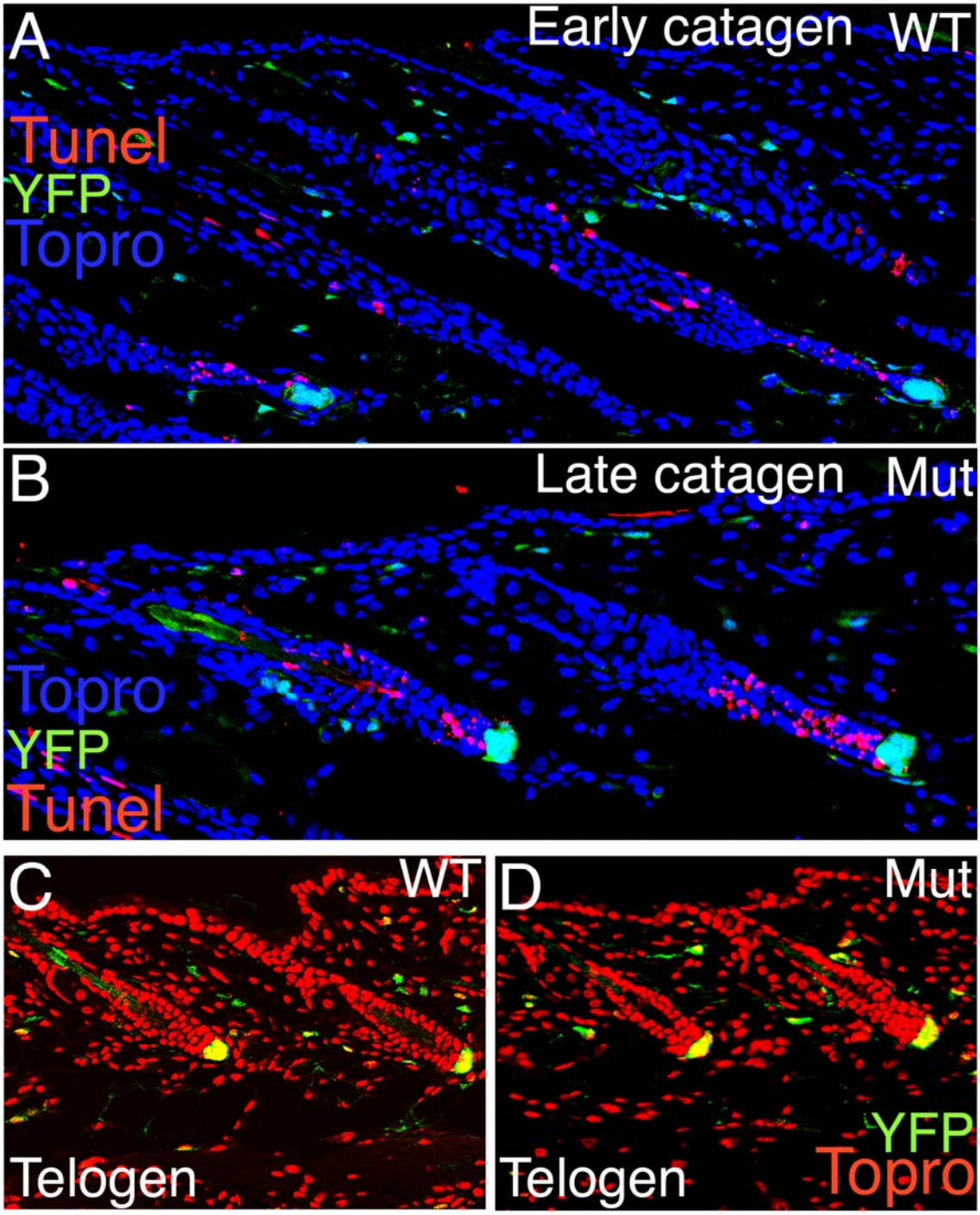

Figure S3. DP-structure during the transition from catagen to telogen remains unaltered in DP lacking β-catenin (related to Figure 4)

In A and B, TUNEL staining of wild type (A) and mutant (B) skins are shown. Nuclei-blue, YFP-green, TUNEL-red. Note the abundance of apoptotic cells in the keratinocyte compartment and their absence in the DP in both wild type and mutant mice. (**B**) Even during late stages of the regression phase when the DP is drawn up towards the permanent portion of the follicle and largely lacks the constraints of the epithelial strand, DP cells remain attached as a compact group of cells with no signs of disintegration or

loss of adhesion properties. (**C-D**) DP structure of mutant telogen follicles (C) is apparently normal and similar to wild type (D).

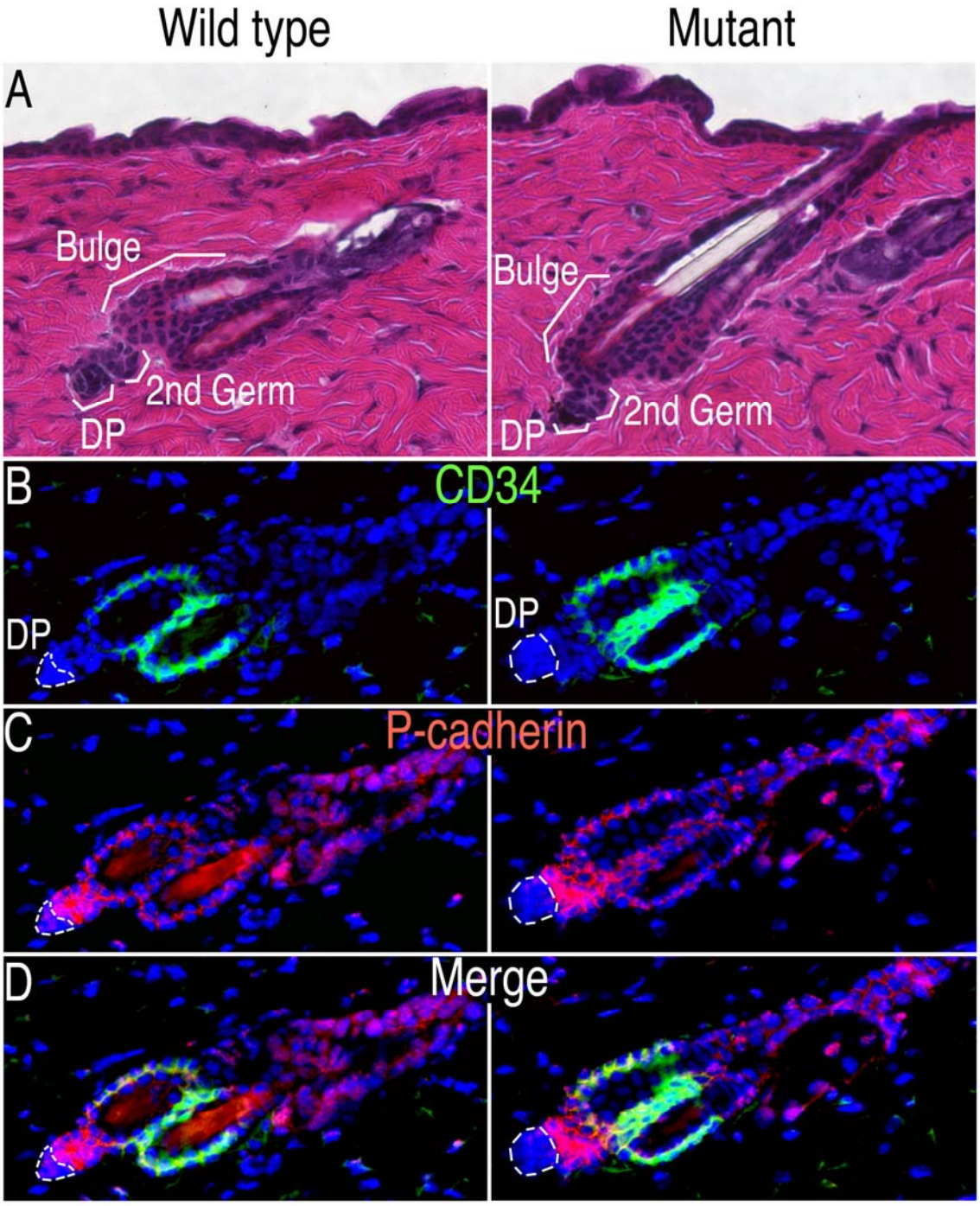

Figure S4. The permanent portion of telogen follicles in mutant mice is apparently normal

(A) Hematoxylin and eosin staining of P50 skin sections during the long, second telogen from wild type and mutant mice. Note the normal morphology of the mutant follicle with a secondary germ in physical contact with and physically separating the bulge and DP compartments. (B-D) Immunostaining for CD34 (B) and P-cadherin (C) of the same hair follicle. In D, a merge of B and C. Blue- Dapi (nuclei).

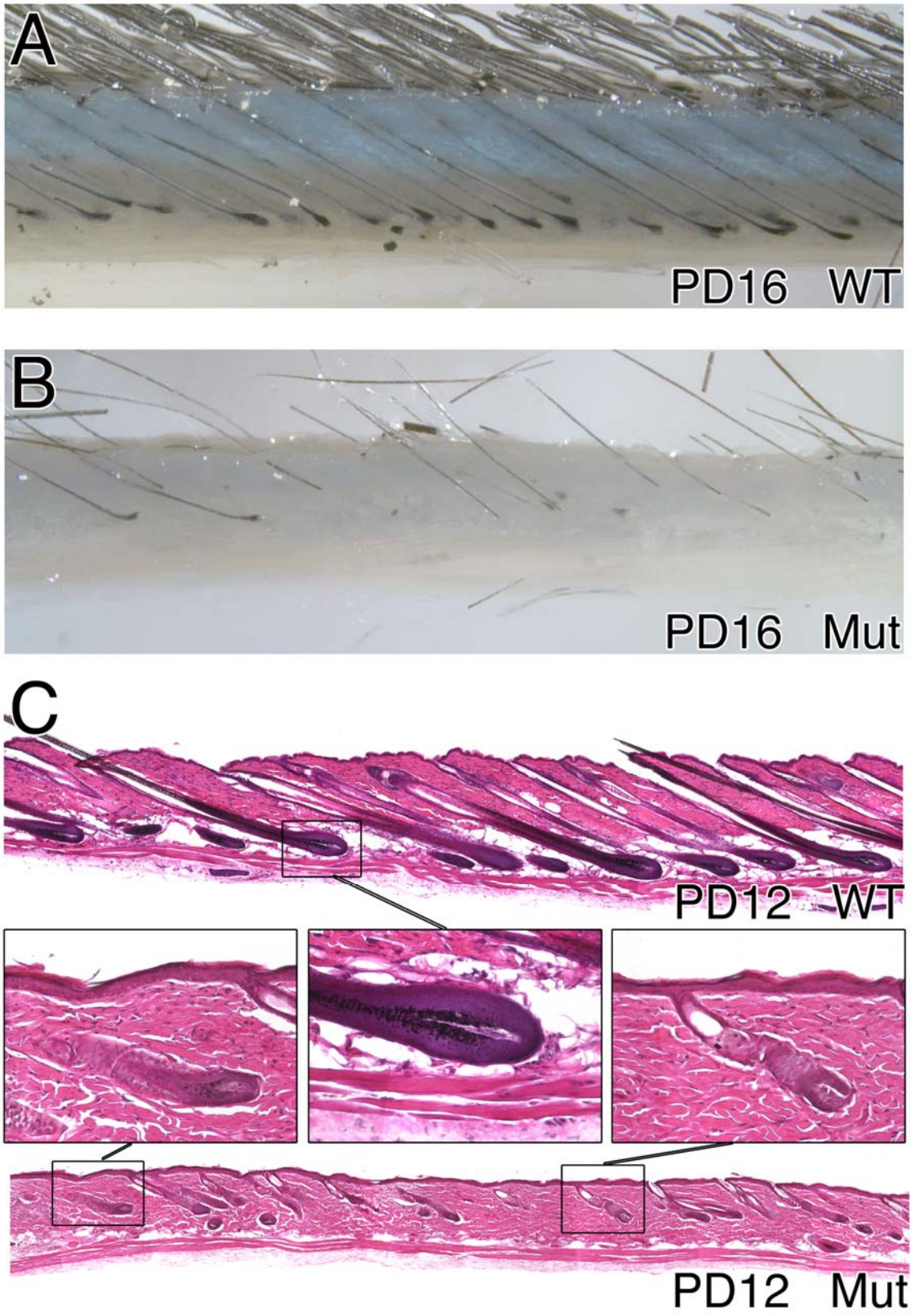

Figure S5. Regeneration is also defective when depilation was employed to provide an anagen-inducing signal (related to Figure 5)

(**A,B**) Side views of wild type (A) and mutant (B) skins 16 days post depilation. (**C**) Hematoxylin and eosin staining of wild type (upper panel) and mutant (lower panel) skin

sections 12 days post depilation. Middle panels are higher magnifications of the corresponding frames in upper and lower panels.

Supplemental Experimental Procedures

Mice. *ROSA26 YFP* reporter (*r26YFP*), *β-actin cre*, and conditional knock-out allele of *β*-catenin (*Ctnnb1*$^{Flox/Flox}$) strains were obtained from F Costantini (Columbia), G Martin UCSF, and Jackson Labs respectively. The DP-specific Cre (*Cor-cre*) mouse was generated by inserting sequences of Cre recombinase into the Corin locus. To detect Cre activity, DPcre/+ mice were bred with r26YFP/+ mice. A knock-out allele of *β*-catenin (*Ctnnb1*$^{Del/+}$) was generated by crossing the floxed allele (*Ctnnb1*$^{Flox/Flox}$) to the *β-actin cre* line. Mice of the genotype *Cor-cre /Cor-cre;Ctnnb1*$^{Del/+}$ were crossed with mice of the genotype *Ctnnb1*$^{Flox/Flox}$*;r26YFP/r26YFP* to generate mice deleted for ß-catenin and expressing YFP specifically in the DP. The genotype of mutant progeny was *Ctnnb1*$^{Del/Flox}$*; Cor-cre /+;rYFP/+*, and littermates of the genotype *Ctnnb1*$^{Flox/+}$*; Cor-cre /+; rYFP/+* were phenotypically wild type.

Histology and immunostaining. Mid-dorsal skins were harvested, fixed in 4% paraformaldehyde, dehydrated with sucrose and embedded in OCT. To detect YFP expression, frozen sections were post fixed with 4% paraformaldehyde and incubated with TO-PRO-3 (1:40,000) to label nuclei. Confocal imaging was carried out with a Lieca imaging system. To detect K14, 8um frozen sections were post fixed in 4% paraformaldehyde, incubated with rabbit polyclonal anti-K14 antibody (1:200) for 1 hour at room temperature and reacted with donkey anti-rabbit secondary antibody conjugated with TRITC in the presence of TO-PRO-3 for 1 hour. To detect CD34 and Pcadherin, fresh frozen skin sections were incubated with rat monoclonal anti-Pcadherin antibody (1:200, R&D), followed by anti-rat secondary antibody conjugated with TRITC and subsequently reacted with rat monoclonal anti-CD34 antibody (1:30) directly conjugated with FITC (BD Biosciences). To reveal skin morphology, hematoxylin and eosin or hematoxylin only staining was performed according to standard protocols.

Hair shaft analysis. Hairs were plucked at the end of the first cycle at P20 and mounted on slides with a thin layer of Gelvatol. At least 200 hairs per mouse were scored for hair-type using 9 wild type and 9 mutant mice. Awl hairs were also specifically scored for the number of medulla columns at the thickest region. Pictures of hair-portions were taken at 100X and 200X on a Nikon Eclipse E800 microscope using a RT Slider Spot camera. For each hair segment, brightfield and phase contrast images were taken. In Photoshop, the phase contrast image was overlaid on the brightfield image at 30% opacity and merged. To generate the whole-hair images, the 100X merged images of hair segments were compiled into one picture and flattened.

TUNEL analysis. To detect apoptotic cell death at single cell level, the In situ cell death detection kit was used (Roche). Mid dorsal skins were harvested, fixed in 4% paraformaldehyde and embedded in OCT compound. Frozen sections were used for the TUNEL reaction to label DNA strand breaks and TMR red conjugated nucleotides incorporated in nucleotide polymers were detected by fluorescence microscopy. For scoring the number of apoptotic cells in a hair follicle the following considerations were included. During anagen, high level of apoptotic events were detected in the upper third of the follicle, probably as part of the differentiation program of this region. The scoring

includes different hair-cycle stages and thus follicle morphology varies substantially. Therefore, as a general guideline, the bottom of the hair shaft was used as the upper limit and Tunel positive cells below that limit were scored. In catagen and telogen the upper limit was simply the proximal edge of the hair club while during anagen, this limit was defined as the border in the bulb area where disorganized keratinocytes become arranged into the medulla columns. Only follicles in which the bottom part of the hair shaft and the DP could be clearly identified were scored. DPs were identified both morphologically and by YFP expression. At least 100 follicles per mouse were scored and the number of mice per stage per genotype was as follows: P10WT/Mut-3/3, P12WT/Mut-4/5, P14WT/Mut-3/4, P16WT/Mut-7/6, P19WT/Mut-4/5.

BrdU analysis. Mice at P10 were injected i.p. with BrdU (100ug/g body weight) (Molecular Probes). 30 min later, mid-dorsal skins were harvested, fresh-frozen and embedded in OCT. Skin sections were fixed for 10min in 1:1 acetone/methanol (v/v) at -20°C, denatured in 2N HCl and incubated with anti-BrdU antibody (1:40) conjugated with Alexa Fluor 546 (Molecular Probes) for 2 hours. Brdu incorporation was detected by fluorescence microscopy and BrdU-labeled cells were scored as follows. Only Brdu-labeled cells in the bulb region were scored using the border between the highly organized medulla structure and the preceding disordered matrix keratinocytes as the upper limit. Only follicles with a clearly visible, morphologically-identified DP were scored. 3 wild type and 3 mutant mice were used and about 30 follicles per mouse were scored.

Cell sorting, genotyping and real-time PCR. To obtain a single-cell suspension, whole back skins were incubated in 0.25% trypsin at 4°C overnight, minced and stirred for 1 hour in 0.2% collagenase at 37°C. YFP-positive cells were FACS sorted twice. Purities of about 75% and 95% were obtained after the first and second sort respectively. To prepare RNA or genomic DNA from sorted cells, the "RNeasy Plus Micro kit" (Qiagen) and "QAIamp DNA investigator kit" (Qiagen) were used respectively. For genotyping, YFP-positive and YFP-negative cells were sorted from the same individual mouse. The YFP-negative cells were used as control for lack of excision. To detect the different alleles of *β-catenin* gene, the following primers were used: RM41 (AAGGTAGAGTGATGAAAGTTGTT-3'), RM42 (CACCATGTCCTCTGTCTATTC-3'), RM43 (TACACTATTGAATCACAGGGACTT-3'). PCR reactions were normalized to contain similar levels of genomic DNA using primers specific for the *Cor-cre* allele (GAAGGTTGGTAGAGTGATTGCC-3' and GGCTTCGGCCAGTAACGTTAGG-3'). For gene expression analysis, 8 P9 mice per genotype from 4 different litters were used individually to sort for DP-YFP positive cells. To prepare cDNA, total RNA was reverse transcribed using random hexamer primers and SuperScript III First-Strand synthesis system (Invitrogen). For real-time PCR, primer pairs for *β-actin* (SuperArray, PPM02945A), *Axin2* (SuperArray, PPM05474B), *Tle1* (SuperArray, PPM37125B), *Nkd1* (SuperArray, PPM05451C), *Nkd2* (SuperArray, PPM05461A), *Sfrp2* (SuperArray, PPM03616C), *Wif1* (SuperArray, PPM04749B), *Notum* (SuperArray, PPM42132A), *Tle2* (SuperArray, PPM28559B), *Fgf10* (SuperArray, PPM03045A), *Hhip* (SuperArray, PPM03498B), *Fgf7* (SuperArray, PPM03104A), *Grem2* (SuperArray, PPM04493A), *Id2* (SuperArray, PPM04420B), *Hoxa9* (SuperArray, PPM25158E), *Zic1* (SuperArray, PPM41395A), *Lef1* (SuperArray, PPM05441E), *Trps1* (SuperArray, PPM26289A), *Sox2* (SuperArray, PPM04762E), *Serpine2* (SuperArray, PPM24913A), *Prss12* (SuperArray, PPM25523A), *Wnt5a* (SuperArray, PPM04748B), *Pdgfra* (SuperArray, PPM03640C),

Igfbp3 (SuperArray, PPM03820E), *Igfbp5* (SuperArray, PPM05198A), *Ngfr* (SuperArray, PPM04327E), *Bmp6* (SuperArray, PPM04429E), *Nog* (SuperArray, PPM04443A), *Alx4* (SuperArray, PPM25333A), *Bmp4* (SuperArray, PPM02998E), *Akp2* (SuperArray, PPM03155A), *Alx3* (SuperArray, PPM25569A) were employed using iCycler thermal cycler (BioRad), MyiQ Single-color Detection system, MyiQ Optical System Software and CYBR Green/Fluroescein PCR Master Mix (SuperArray). Differences between samples were quantified based on the ΔΔCt method.